GeoPlanning
Journal of Geomatics and Planning
Vol. 9, No. 2, 2022

e-ISSN: 2355-6544

Received: 01 October 2022;
Accepted: 29 November 2022;
Published: 08 December 2022.

**Keywords:**
coastal development, Padang City, coastline instability, coastal erosion, and morphological alteration

*Corresponding author(s)
email: ulun002@brin.go.id

*Original Research* Open access

# Assessing Urban Development Impacts in the Padang Coastline City, West Sumatra Indonesia; Coastline Changes and Coastal Vulnerability

Ulung J. Wisha [1,2]*, Ruzana Dhiauddin [3], Koko Ondara [2], Wisnu A. Gemilang [3], Guntur A. Rahmawan[3]

1. *Physical Oceanography Laboratory, Department of Physics and Earth Sciences, University of the Ryukyus, Japan*
2. *Research Center for Oceanography, National Research and Innovation Agency (BRIN), Indonesia*
3. *Research Institute for Coastal Resources and Vulnerability, Ministry of Marine Affairs and Fisheries, Indonesia*

DOI: 10.14710/geoplanning.9.2.73-88

## Abstract

The capital coastline city of Padang is intensively developed to enhance tourism attractions and protect the coastline from natural hazards and disasters. Massive urban developments applied in the coastal area have not gone well, and several regions have been eroded and unstable. This study aimed to determine the significant change in Padang city's coastline due to rapid urban development in the coastal area. Spatial analyses are employed to determine the coastline changes and coastal vulnerability, such as a DSAS (Digital Shoreline Analysis System) and Smartline-associated CVI (coastal vulnerability index) approach. A hydrodynamic and coastal model is also used to illustrate the transport mechanism and predict the level of coastal erosion. The result shows that substantial coastal changes and vulnerability have occurred. Of particular concern, 77.21 % of Padang's coastline is eroded with a rate of 0.21 - 49.4 m/year, 10.46% stable, and the rest, 12.32% experiencing accretion. More than 9% of coastal areas are categorized as highly vulnerable. The hydrodynamic-based model confirms the coastal erosion in several significant areas in Padang City, proven by the relatively high value of bed-level change (ranging from 0.39 up to -4 m) and considerable variability of seasonal sediment transport and suspended materials. The erratic hydrodynamics and ineffective coastal building are the primary factors triggering Padang City's coastal instability.



## 1. Introduction

Padang Coastline City is geographically positioned on the west coast of Sumatra, Indonesia, with a coastline of 84 km. The general city area is 694.96 km$^2$; more than 60% of that area is protected forest, and the rest are functional urban areas. The topography state of Padang City varies; 49.49% of the site is situated in the slope area, and around 23% is the declivous area. Padang City faces the Indian Ocean in the west, below the equator, and between Eurasian and Indo-Australian Plates boundaries (Ramdhan, 2021). This state makes Padang City prone to coastal hazards and disasters (Gemilang et al., 2017). That is why the government has rebuilt and rehabilitated the coastal protections since 2010. On the other hand, 25% of Padang City is a built-up area. The developments in the coastal zone have been occurring because of tourism interest.

The rapid urban development applied in Padang City without any scientific assessments impacts the other area nearby on unstable coastal erosion and sedimentation. As a result, several regions are eroded, as reported

in Padang Beach, northern Padang, and within the Bungus Teluk Kabung area (Figure 1). Those areas are significant as the center for government buildings, department stores, tourism, port, schools, and universities. Supported by unstable geological settings, coastal erosion is undoubtedly avoided. Indeed, change in the coastal area is always undergone, and it will be stable naturally without any significant artificial interventions. Therefore, making a substantial development without any scientific reason in the coastal area will worsen the condition.

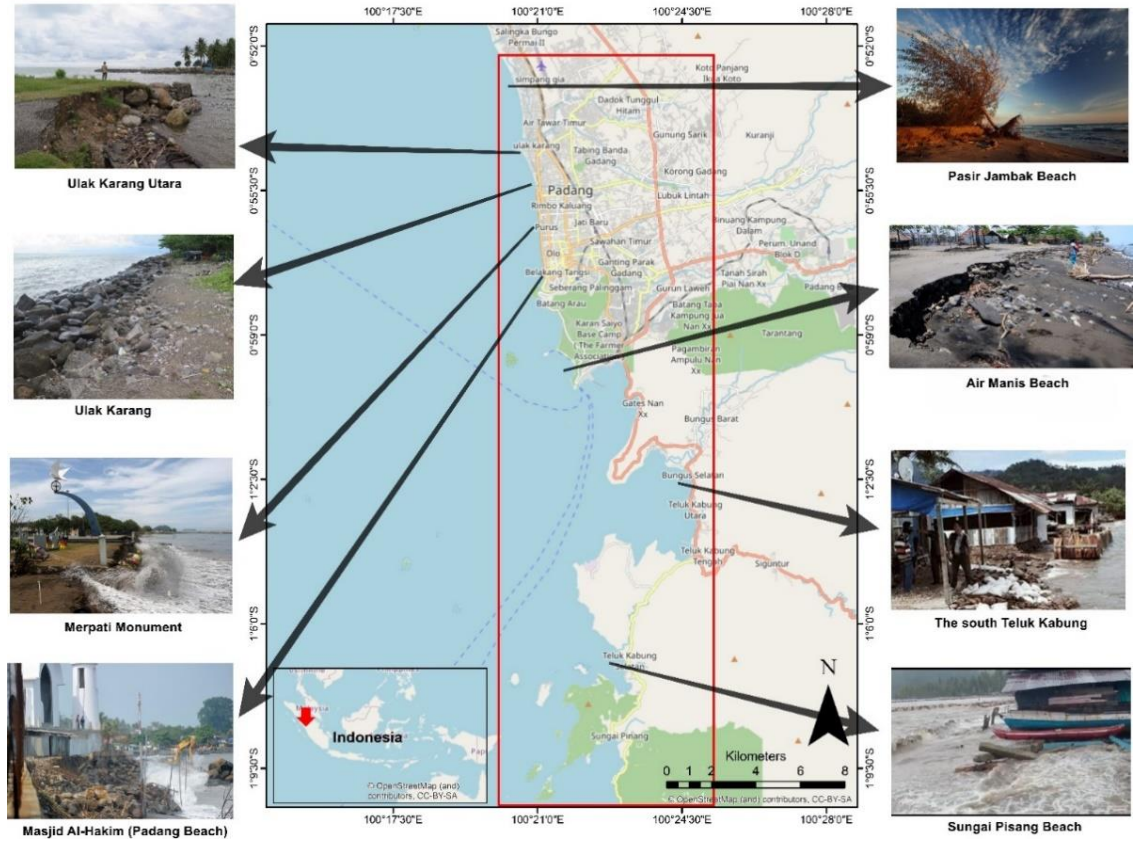


*Source: Analysis, 2022*

**Figure 1**. The coastal areas impacted erosion throughout Padang Coastline City; red square denotes the area of study

Padang coastal area comprises alluvial properties arranged by coarse sand and mud throughout the coastline with a topography profile ranging from 0 to 10 m above sea level (Fajrin et al., 2021). Ocean wave exposure mainly triggers the dynamics of the Padang coastline (Rizal & Ningsih, 2020). To date, the report of coastal erosion cases is still skyrocketing. According to Haryani & Syah (2018), erosion on the Padang coastline is triggered by waves-induced longshore currents. At the same time, the accretion concentrated in the estuarine areas is caused by silting and river flow changes. Determining the causal factors triggering coastal processes is crucial since coastal instability is undergoing in Padang City.

Coastline change and vulnerability in Padang City should be studied more. Moreover, the local news published many reports regarding erosion occurring along the coastal area. The speed of coastal erosion in Padang City has been reviewed by Fajri & Tanjung (2012), but this study only focused on the three observation stations in the Padang Barat Sub-district. The effectiveness of coastal building in Padang Beach was also revealed by Wardani et al. (2019). Yuhendra et al. (2019) calculated the erosion in Air Manis Beach by approximately 50 m. The effects and adaptation to coastal vulnerability in Padang City have been reported by (Ramdhan, 2021), describing the disaster and climate change threats and the adaptation adopted by the local government. Many

kinds of coastal hazards and disasters threatening Padang Coastline City have also been described (Gemilang et al., 2017; Oktiari & Manurung, 2010; Putri et al., 2018; Tohari et al., 2011).

The previous studies only report erosion in one or two significant areas over the Padang coastline. The coastline change identification needs to be updated accurately. A regional survey identifying coastline change throughout the coastline area of Padang City is essential since rapid urban developments have been applied, and coastal erosion cases are still reported (Hakam et al., 2019; Yuhendra et al., 2019). This study analyzes the ten-year coastline changes by employing the DSASv5 and a modified Smartline method to assess the 14 chosen physical factors triggering the susceptibility level in the coastal area. On the other hand, a hydrodynamic model simulating the longshore-current patterns and predicting the level of erosion and sedimentation should be carried out. No reports describe the coastal morphological alteration and modeling to date, and these aspects should be investigated. However, the information on coastal vulnerability is significant for the local and central government in future decision-making for early mitigation, physical support, and future regional development. This study aims to determine the coastline changes, assess the vulnerability level, and estimate the possible future alteration along the Padang City coastline.

## 2. Data and Methods

### *2.1. Study Site*

The study area is focused on the Padang City coastline, West Sumatra, Indonesia (Figure 1). Generally, the coastal area of Padang City is structured by alluvial compositions arranged by coarse sand and mud sediment within a declivous slope (Gemilang et al., 2017). The wave regimes from the open ocean provenance influence the dynamics of the coastal area. The erosion predominantly occurs along the coastline detected in the upstream regions, proven by the high sediment supply flowing through the river and settling in the surrounding estuaries (Hakam et al., 2019). The variability of wave-driven current is believed to be the primary factor triggering coastal instability in Padang City. 146 observation points within six subdistricts (Koto Tangah up to Bungus Teluk Kabung) have been observed directly in the field (Figure 2). This survey was conducted during April and August 2019.

Geologically, the coastal area of Padang City is composed of igneous rock, sediment, and soft-type sediment. The formation of the coastal area is related to the beach constituent materials because the study area is composed of compacted sediment associated with cliff materials resulting in the declivous hilly formation. The coastal elevation in Padang City is divided into three segments: elevation >25 meters observed along 4 km between Lubuk Begalung and Bungus Teluk Kabung; elevation of 4-10 m found throughout the coastline, except for Padang Barat Subdistrict with 0-3 m elevation. On the other hand, the slope of Padang City ranged from 1-13% identified along 63 km from Koto Tangah up to Bungus Teluk Kabung Subdistrict (Tanto et al., 2017).

Even though artificial coastal protection triggers unstable sediment transport, it might protect the coastal area from disasters and hazards. That is why along 29 km (39%) of coastline in Koto Tangah, Padang Utara, Padang Barat, Padang Selatan up to Bungus Teluk Kabung Subdistricts is protected by natural greenbelt and artificial coastal protection. On the other hand, almost 52.5 km from Koto Tangah up to Padang Selatan Subdistrict is used as a settlement area. In contrast, the Bungus Teluk Kabung Subdistrict is commonly used as the center for industrial and fisheries interests (Gemilang et al., 2017).

### *2.2. Field Data Collection*

The field data were collected via direct field survey and secondary data modeling. We employed a Smartline technique (Lins-de-Barros & Muehe, 2013; Sharples et al., 2009; Thom et al., 2018) with several modified parameters according to the nature of the study area. Direct observation of the eleven chosen parameters (beach materials, geomorphological states, wave exposure, beach slope, wave height, sediment grain size, distance between coastal to the prone area, coastal berm, beach face features, land use, and coastal building condition) was performed. On the other hand, the modeled parameters were Digital Elevation Model (DEM),

tidal range, and coastline changes. In addition to the observation station, all parameters were collected at specific points at 0.5 up to 1 km.

The data collected were then assessed and classified into five scoring criteria (1 to 5). The given score shows the contribution level for each parameter observed to coastal vulnerability. The scoring classification is shown in Table 1. Parameters used in the scoring category are significant in determining coastal vulnerability. In addition to the field survey, these parameters consideration is based on the preliminary field observation previously performed.

**Table 1.** Physical parameters and their classification in the Smartline Technique

| Parameter | Very low | Low | Moderate | High | Very High | Adapted from |
|---|---|---|---|---|---|---|
| **Score** | 1 | 2 | 3 | 4 | 5 | |
| Beach Materials | Ice | Coral | Hard Rock | Soft Rock | Soft Sediment | Sharples et al. (2009) |
| Geomorphology | Cliff | Stable Beach with Vegetation | Stable Beach without vegetation | Beach | Delta, Swamp, Dune | Jadidi et al. (2013) |
| Wave Exposures | Highly Protected | Protected | Partly Protected | Exposed | Fully exposed | Abuodha & Woodroffe (2010) |
| Slope (%) | 1-13 | 14-20 | 21-28 | 29-35 | >36 | Jadidi et al. (2013) |
| Berm Features | Forest, Pond, Swamp | Rural Area | Mixed Rural Area | Urban Zone | Mixed Urban | Jadidi et al. (2013) |
| Grain Size | Very Fine | Fine | Moderate | Coarse | Very Coarse | Wentworth, (1922) |
| Distance between coastal to the prone area (m) | >61 | 31-60 | 21-30 | 11-20 | 0-10 | Jadidi et al, (2013) |
| The height of Berm | >30.1 | 20.1-30 | 10.1-20 | 5.1-10 | 0-5 | Abuodha & Woodroffe (2010) |
| Beachface Features | Hard Structure | Greenbelt | - | - | Unused area | - |
| Land-use | Protected area | Unclaimed | Settlement | Industrial | Agriculture | Gündogan et al. (2011) |
| Coastal Building Condition | Very Good | Good | Moderate | Need Maintenance | Damaged/ No building | Jadidi et al, (2013) |
| Elevation (m) | >25 | 17-24 | 11-17 | 4-10 | 0-3 | Jadidi et al, (2013) |
| Tidal Range (m) | <1 | 1-1.9 | 2-4 | 4.1-6 | >6 | Jadidi et al, (2013) |
| Coastline Changes (m/year) | Accretion (>2.1) | Stable (1-2) | Stable (-1 - +1) | Erosion (-1 - -2) | Highly Eroded (<-2) | Abuodha & Woodroffe (2010) |

*Source: Analysis, 2022*

### *2.3. Digital Shoreline Analysis System (DSAS)*

A coastline changes analysis was performed to determine alterations resulting from the intense urban development level in Padang City. Many cases of coastal erosion have been reported and getting worse, especially in vital areas. Digital Shoreline Analysis System (DSASv5) was employed to estimate the coastline changes throughout Padang coastal area. DSAS enables the user to calculate rate-of-change statistics from multiple time series shoreline positions (Himmelstoss et al., 2018). The two main components, coastline and baseline are

preconditions to process the DSAS analysis (Wisha et al., 2021). Additionally, automated measurement transects, and metadata are needed in the form of shapefiles recording the distance between the historical coastlines crossed by this transect line. By combining these components, we could calculate the coastline changes spatially.

This study compared Landsat 8 OLI imagery recorded in 2009, 2014, and 2018. These images were digitized precisely following the coastline patterns. This stage was done manually by applying on-screen digitation. The baseline and coastline from north to south of Padang City were digitized successively. The transect length was approximately 500 meters with 10 - 100 m intervals (Figure 2). Then, the Linear Regression Rate (LRR) method was used to predict and classify the rate of coastline changes through the change statistics window in DSAS (Dada et al., 2019). This method is a statistical analysis for counting the level change applying linear regression that can be determined using a least-square regression line toward intersection points of coastline with transects (Himmelstoss et al., 2018). However, the linear trend was estimated by fitting a regression line to the coastline positional data as follows:

$$Y = mX + B \quad [1]$$

where:
$Y$ = the predicted coastline positions
$m$ = the rate of coastal movement
$X$ = the date
$B$ = the intercept

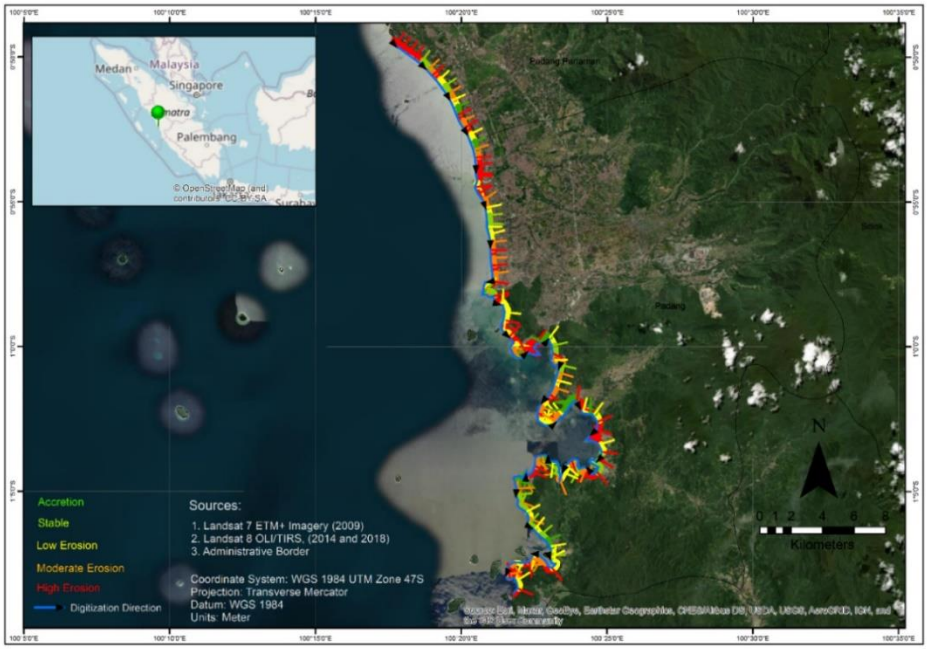


*Source: Analysis, 2022*

**Figure 2**. The transect of Smartline Observation and DSAS Calculations

This expression was applied on all 146 transects to process the linear regression for each transect. The next stage was mapping the coastline change rate by attaching change statuses on the most recent data. The classes are erosion, accretion, and stability. In this step, cutting the latest data (2018) with an interval of 100 m given a status based on LRR was needed. These processes must adhere to the direction of baseline digitation. The level of coastline changes was classified into four classes as follows:

Accretion = if the rate is >2 m/year

Stable = if the rate is between >1 and ≤ 2 m/year
Low erosion = if the rate is between >-1 and ≤ 1 m/year
Moderate erosion = if the rate is between >-2 and ≤ -1 m/year
High erosion = if the rate is ≥ -2 m/year

In this analysis, we applied the high-water line (HWL) as the preferred indicator for coastline delineation because of its ease of interpretation and field location (Roy et al., 2018). HWL is the line attached to the land up to the line reached by the highest water level during the spring tides phase. Even though many factors should be considered in determining the horizontal location of the mean high-water line due to the dynamics of beach and foreshore, the use of HWL is the best reference for locating the boundary between land and sea within an unstable environment (Mandal et al., 2020).

### *2.4. Coastal Hydrodynamics and Sediment modeling*

We employed a coupled model of MIKE21 with flexible mesh to simulate the mutual interaction between waves and currents using a dynamic coupling between the hydrodynamic and spectral wave models (Wisha et al., 2018). Hence, full feedback on the bed level changes calculated from the coupled model could be included. We sampled the result from the coupled model developed according to the significant eroded coastal zones shown in Figure 1. The estimated erosion (sedimentation) was determined as the bed level changes resulting from the simulation. Furthermore, the spatial distribution of estimated erosion was also mapped.

The sediment transport model adopted in this study is based on the hydrodynamic models previously simulated (Flow and Spectral Wave). The following equation defines the correlation between the wave energy flux component and the sediment transport:

$$W_{ef} = \frac{\rho g}{8} H_b^2 C_b sin\alpha_b cos\alpha_b \qquad [2]$$

Where:
$W_{ef}$ = Wave energy flux component along the coast at the time of wave breaking ($kg.m.s^{-1}$)
$\rho$ = Specific gravity (seawater) ($kg.m^{-3}$)
$g$ = Gravity acceleration ($9.81\ m.s^{-2}$)
$H_b$ = Wave Height at the time of breaking ($m$)
$C_b$ = Breaking wave celerity ($m.s^{-1}$)
$\alpha_b$ = Breaking wave angle

A formula established by Triatmodjo (2012) was used to estimate the annum sediment transport. This formula can be applied to the homogenous sandy beach with a grain diameter ranging from 0.175-1 mm. This formula is suitable to use in the Padang coastal area, whereby the sand sediment predominates along the Padang coastline (Hakam et al., 2019). The formula is defined as follows:

$$Q_s = \frac{K}{(\rho_s - \rho)g(1-n)} W_{ef} \qquad (3)$$

Where:
$Q_s$ = Sediment transport along the coast ($m^3.s^{-1}$)
$K$ = 0.39
$\rho_s$ = Specific gravity (sand) ($kg.m^{-3}$)
$n$ = Porosity ($n \approx 0.4$)

A TSS (total suspended sediment) modeling technique previously established for coastal and estuarine zones was simulated (Wisha et al., 2022b). This simulation estimates the monthly averaged suspended sediment concentration along the Padang coastline, particularly after the urban development has been applied. This simulation is based on the flow model previously simulated and validated by field measurement in 2019. This model included the bed and suspended loads calculated separately. In addition to the resume of research methodology, this study framework is shown in Figure 3.

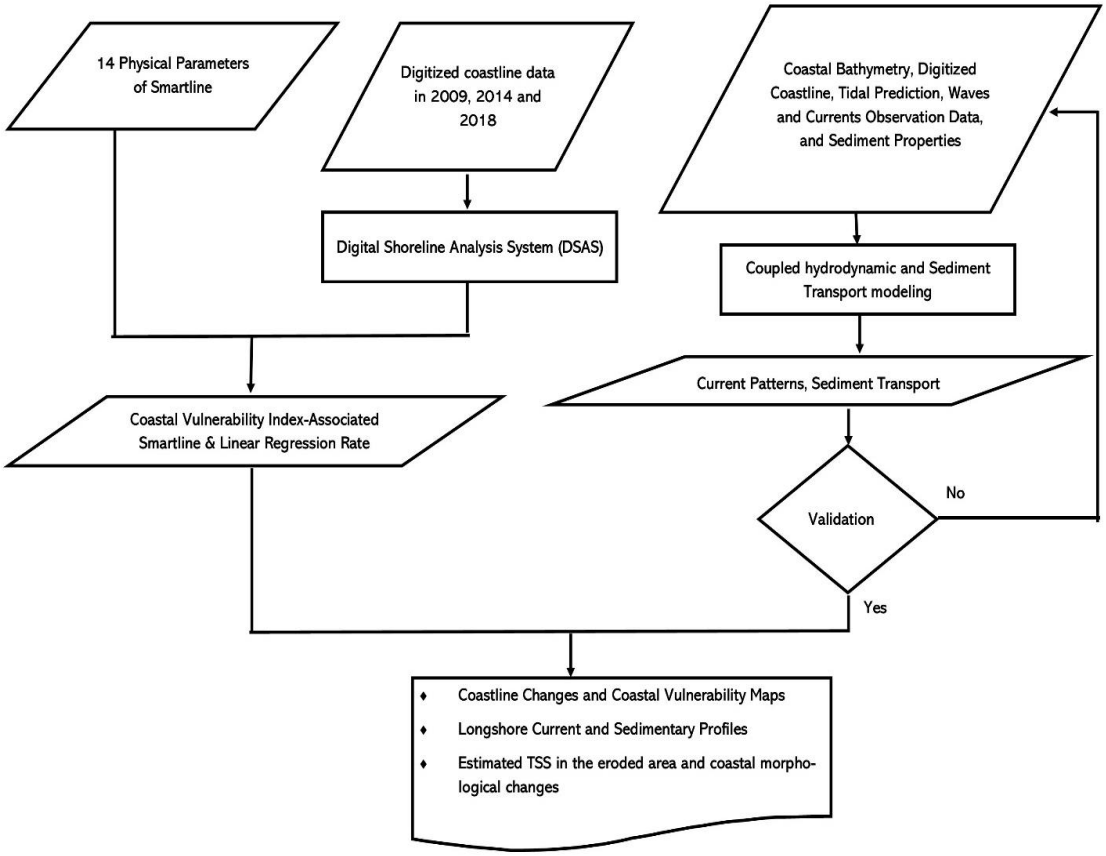


*Source: Analysis, 2022*

**Figure 3.** Research frameworks of the spatial and hydrodynamic modeling

## 3. Result and Discussion

### 3.1. *Coastline Changes of Padang City*

Based on 10-year compared data, the coastline changes in Padang City were sufficiently dynamic, wherein the coastal erosion was predominant with almost 77.21 % of eroded areas and a rate of 0.21 up to 49.4 m/year (Figure 4a). The erosion level is divided into three classes: highly eroded coastline 33.34%, moderately eroded coastline 20.58%, and lowly eroded 23.28%. The remnant classifications were accretion and stable, with 10.46% and 12.32%, respectively.

We identified that 33.34% of Padang City's coastline was highly eroded wherein the coastline retreated by more than two m/year over ten years. Ironically, except for the Padang Utara Subdistrict, only 9 km (12 %) of the stable coastal area was identified in all observed subdistricts. In contrast, it was only 7.7 km of the accreted area identified with an approximate rate of 2 m/year.

A significant coastal erosion in Lubuk Begalung Subdistrict was detected with a rate of approximately -49.4 m/year (Figure 4b), specifically between Air Manis Beach and Bayur Bay. This result confirms the previous study (Yuhendra et al., 2019) that the highest coastal erosion is observed in Air Manis Beach, with a 50-m estimation of vanished coastline. The unclaimed coastline was observed in several parts of Sungai Pisang. On the other hand, the most nourished beaches were identified along Lubuk Begalung up to Bungus Teluk Kabung.

Besides Lubuk Begalung, the most eroded areas were the Padang Barat and Bungus Teluk Kabung Subdistrict (Sungai Pisang and Bungus Selatan). Many urban developments in the coastal area have been applied in the Padang Barat Subdistrict, such as the Merpati monument and Masjid Al-Hakim, where overwhelming erosion is previously reported. On the other hand, Sungai Pisang and the Bungus Selatan Village are on the same page, where a tendency of coastal erosion was also observed. The coastline instability and erosion have threatened the city's vital infrastructures, where the center of economic activities, government offices, industries, and settlements are located. The existence of coastal building and protection probably plays a significant role in inducing coastal instability, which will be more addressed in the next section.

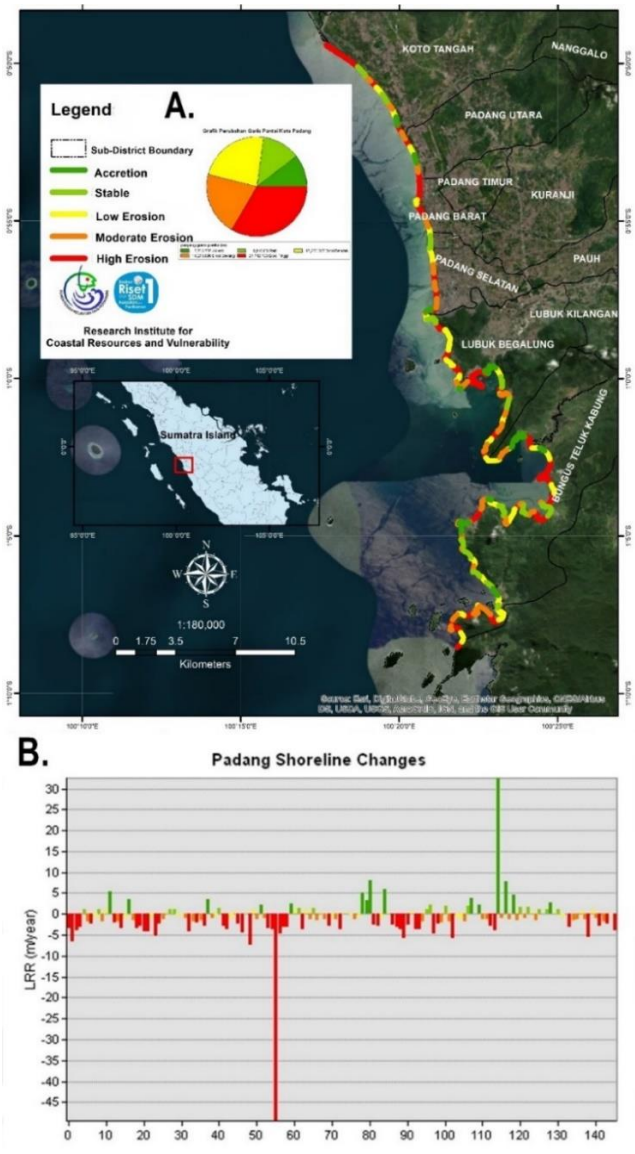


*Source: Analysis, 2022*

**Figure 4**. (a) Coastline changes in Padang coastline over ten years of observation and (b) the alteration rate at each transects

According to Hakam et al. (2019), the coastal erosion issue in Padang Barat Subdistrict commenced in the early 1800s because of the coastal barrier (Mount Padang) hampering the southerly sediment transport. Since then, the development of the coastal groin had applied without any preliminary studies regarding ocean currents and waves. Despite supporting marine tourism and coastal protection projects, the construction of coastal buildings triggers the alteration in sediment supply and demand transport patterns, resulting in erosion in nearby areas.

Besides experiencing extensive erosion, silting and sedimentation were also found in several areas, such as Koto Tangah, a tiny part of Lubuk Begalung, and some areas of Bungus Teluk Kabung. The highest accreted area was in the surrounding PLTU Sirih Bay (within Bungus Teluk Kabung subdistrict), with a maximum rate of approximately 35.1 m/year (Figure 3b). According to Gemilang et al. (2017), the southern part of the Bungus Teluk Kabung Subdistrict is accreted at a rate of 3-9 m/year.

### 3.2. *Coastal Vulnerability of Padang Coastline City*

Based on the scoring on the considered parameters, the CVI index of Padang Coastline City ranged from 16.6 – 1096.3, divided into five classes of vulnerability: very low vulnerability (16.6-232.6), low vulnerability (232.7-448.6), moderate vulnerability (448.8-664.7), high vulnerability (664.8-880.7) and very high vulnerability (880.8). 40% of the coastal area of Padang City is categorized into very low vulnerability, situated in the Koto Tangah and a tiny part of Bungus Teluk Kabung (Figure 5).

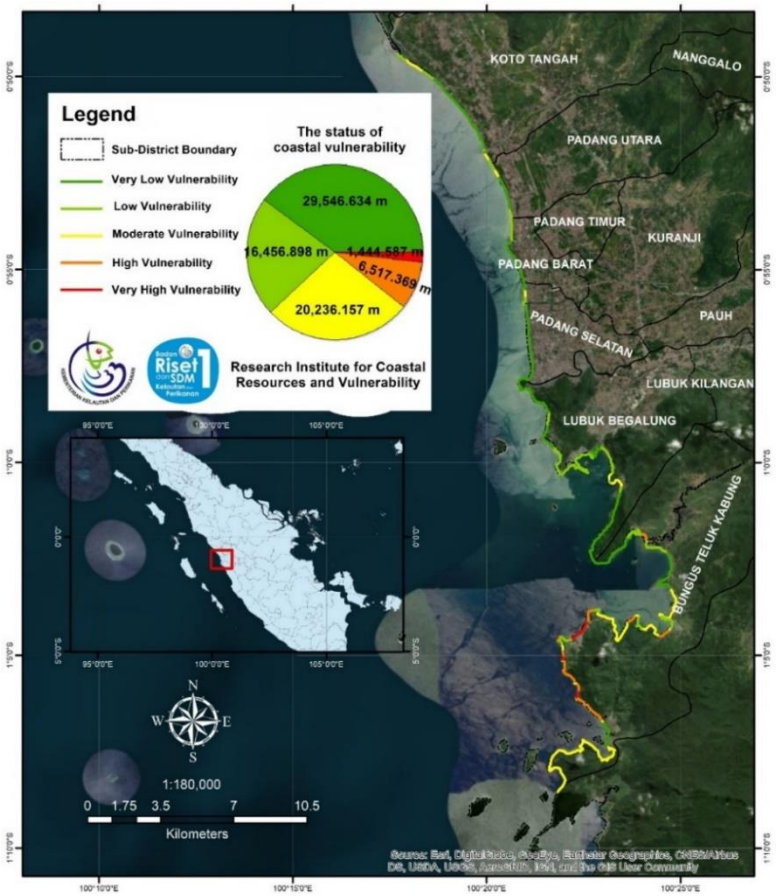


*Source: Analysis, 2022*

**Figure 5.** Coastal vulnerability map of Padang coastline

Overall, almost the northern coastline of Padang City is predominated by very low up to moderate vulnerability, where the coastal formation and protection decrease the potency of being vulnerable. In contrast, high vulnerability is observed in the southern coast (a tiny part of Lubuk Begalung and Bungus Teluk Kabung),

generally unclaimed and beachy areas. This result indicates that substantial land use changes could determine a region's vulnerability status. The more significant the alteration and development of a coastal area, the more arduous the nature to balance the changes as provenance, thereby substantially impacting the other nearby areas to get either eroded or vulnerable.

Instead of coastal protection in southern Padang City, anthropogenic activities, such as industrial interest, port development, reclamation, tourism, and other coastal urban developments, are believed to trigger coastal vulnerability significantly (Dada et al., 2019). According to Zhu et al. (2017), besides the influence of human activities on triggering coastal susceptibility, climate change-induced hydrodynamics is the main factor controlling coastal dynamics and vulnerability. Hence, this aspect will be addressed in the following subsection.

The assessment of coastal vulnerability employing a Smartline method is initially applied in Padang City. The coastal vulnerability assessment aims to determine an initial state identifying the prone areas in Padang City. The decision could be quickly made to prevent further planning that can endanger the significant areas. However, a shortcoming of several data employed and qualitative surveys are related to the clarity of the study results because the quality of data and information on several variables could affect the vulnerability scoring and ranking (Dada et al., 2019).

### *3.3. Model-Based Longshore Current Profiles and Estimation of Erosion-Sedimentation*

The monthly average of longshore-current profiles shows a similar trend in all observation stations (Figure 6a). It was generally higher during the northeast monsoon and getting lower during the southwest monsoon, with a deviation of about 0.02m/s. Moreover, the dominant longshore currents flow was influenced by the monsoon system, whereby it tended to move southward during the northeast monsoon and vice versa for the remnant period. In the northern stations (Pasir Jambak, Ulak Karang, Ulak Karang Utara), a similar pattern in velocity was observed, ranging from 0.046-0.06 m/s. In the Padang Barat Subdistrict, the longshore-current fluctuations were sampled at Merpati Monument and Masjid Al-Hakim, where an enormous coastal erosion occurs. The longshore current was more substantial than the northern stations (ranging from 0.05-0.0.07 m/s).

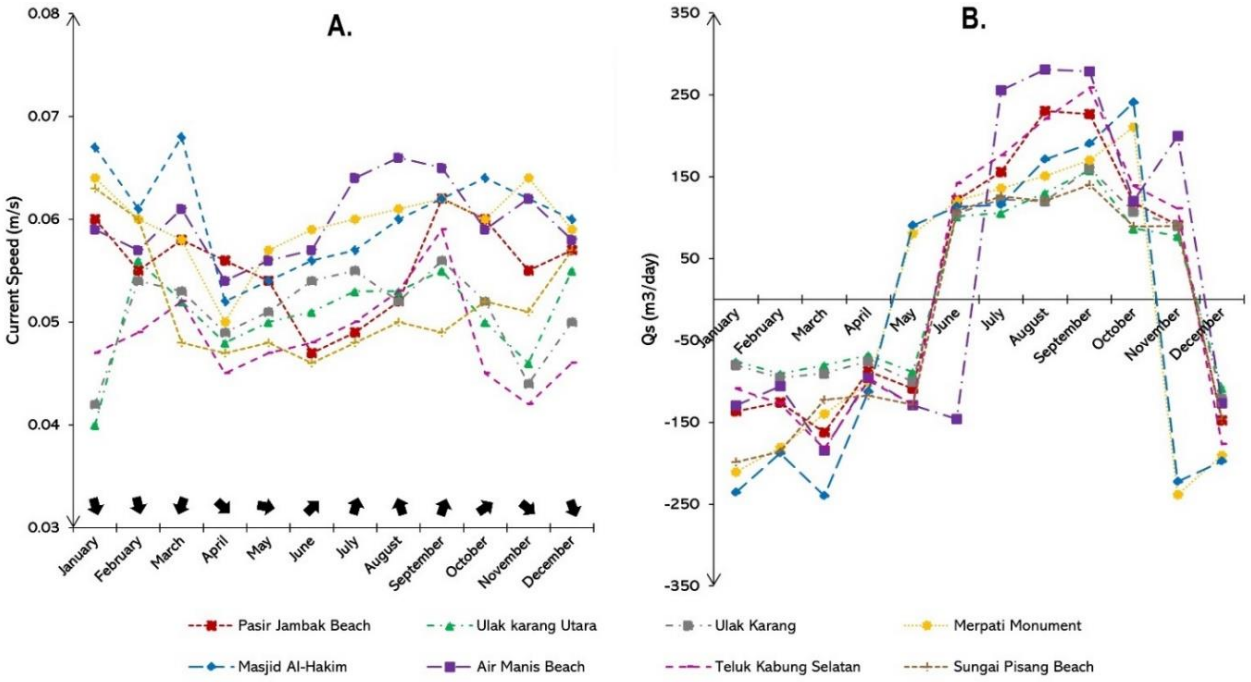


*Source: Analysis, 2022*

**Figure 6.** Monthly average of longshore current profiles (a) and estimated sediment transport (b) in the eroded area of the Padang coastline. Black arrows denote the dominant current direction.

The current velocity in Air Manis Beach ranged from 0.055-0.067 m/s. The moderate-very high erosion in this area is influenced by unstable sediment supply from nearby estuaries. Since the urban development has been applied in the river's mouth, the erosion in another part commenced occurring. This area's relatively strong current also significantly triggers imbalanced sediment transport along the coast (Burnette & Dally, 2018). Additionally, the pressures from anthropogenic activities also result in vulnerable coastal areas (Gemilang et al., 2020).

**Table 2**. Total sediment transport and the dominant transport direction

| Observation station | Sediment flux Qs ($m^3/day$) | Dominant sediment type | Sediment transport dominant direction |
|---|---|---|---|
| Pasir Jambak Beach | 173.982 | Fine-Medium sand | North |
| Ulak Karang Utara | 149.502 | Fine sand | North |
| Ulak Karang | 142.570 | Fine sand | North |
| Merpati Monument | 193.400 | Fine sand | South |
| Masjid Al-Hakim | 274.400 | Fine sand | Southwest |
| Air Manis Beach | 217.404 | Fine sand | Northwest |
| Bungus Selatan Beach | 222.920 | Fine-Medium sand | Northeast |
| Sungai Pisang Beach | 224.830 | Medium sand-silt | Southwest |

*Source: Analysis, 2022*

The remnant observation stations are Bungus Selatan and Sungai Pisang Beach. The longshore currents' profiles were considerably different due to the different morphological settings. In these areas, the gulf formation is supposed to weaken the current movements because of the presence of peninsula formations protecting the bay. The model result showed that the longshore current was relatively calm during the northeast monsoon and stronger during the southwest monsoon, ranging from 0.045-0.06 m/s and 0.047-0.063 m/s for the Bungus Selatan and Sungai Pisang stations. The symptoms of coastal erosion are currently reported because of the absence of coastal protection, substantial changes in land use, and robust hydrodynamic profiles.

The estimated sediment transport in all stations varies considerably (Figure 6b). Except for Pasir Jambak, Air Manis, and Bungus Selatan stations, sediments transport peaked during the second transitional period season-northeast monsoon (September-February), ranging from 75.5-258.32 $m^3$/day. At the Pasir Jambak station, the highest sediment transport was estimated during August at 230.43 $m^3$/day, then significantly decreased during April (87.86 $m^3$/day). Compared to the other stations, the relatively high sediment distribution was observed at Air Manis station ranging from 95.89-280.83 $m^3$/day, reaching its peak level during August, and getting tremendously low during April. Moreover, an anomaly was identified during June, whereby the sediment predominantly moved southward. A complex coastal morphology in Air Manis Beach could be the main factor causing this state. According to Burnette & Dally (2018), the deformed primary direction of wind-wave-driven current due to coastal bathymetry and morphology variation close to the coastal area could occur. At the Teluk Kabung Selatan Station, the sediment transport ranged from 98.83-258.32 $m^3$/day. The high transport was identified during the second transitional season (August-September), while during the remnant periods, the transport was not too high, on average, 132.88 $m^3$/day. In addition to coastal building developments in the study area, the coastal erosion and instability observed throughout Padang coastline are the long-term impact of hydro-oceanographic variability wherein this aspect may be unconsidered while planning and during the construction.

The relatively low sediment transport was identified at the Ulak Karang and Ulak Karang Utara stations, where the attached coastal groins and revetment exist. The presence of coastal protection alters longshore-current features increasing the bed shear stress, thereby inducing a lower mixing and turbulence of nearshore bottom sediment (Pascolo et al., 2018). On the other hand, the relatively high sediment transport observed at Merpati Monument and Masjid Al-Hakim station is due to coastal building-induced longshore current deformation and the increased exposure to wind-wave-driven current (Koropitan et al., 2021). Even though the exposure to waves and currents was sufficiently substantial at Sungai Pisang Beach, the sediment transport was not entirely high because of the cliff formation along the coastline of the southern Bungus Teluk Kabung Subdistrict.

Based on the total sediment transport at the entire observation station, we found that the southern stations have a relatively higher annual sediment transport ranging from 217.404 to 274.400 $m^3$/day (Table 2). Aside from the absence of coastal protection, the increased sediment flux is due to the high exposure of current, substantial urban development in the coastal area, the coastal morphology formation changes, and the dominance of sediment type at every observation station (Khan et al., 2021). According to the field survey, the sediment type was generally river-sourced fine sand sediment. However, sediment mixing (fine and coarse) was identified during high tidal conditions. Furthermore, the presence of coarse fractions indicates a robust current environment (Gemilang et al., 2018).

The total suspended sediment (TSS) was modeled and validated by the field measurement (green dashed line in Figure 7). Overall, the highest suspended sediment concentration was observed at the southern stations (from Air Manis to Sungai Pisang), ranging from 121-157 mg/L, which was not considerably divergent during ebb and flood tides. At the Sungai Pisang station, the highest TSS was identified at approximately 150 mg/L during ebb and flood tides. Besides the fine cohesive sediment predomination, the relatively strong sea current features significantly control the sediment turbulence and mixing (Wisha et al., 2022a). Compared to the other stations dominated by fine-medium sediment, Sungai Pisang Beach tends to have high turbidity resulting from the cohesive sediment resuspension, which requires longer to settle in the sea bottom (Nurdjaman & Putra., 2017). On the other hand, besides the fine sediment predomination, the low TSS concentration (<90 mg/L) observed at the Padang Barat station indicates the weaker current flow.

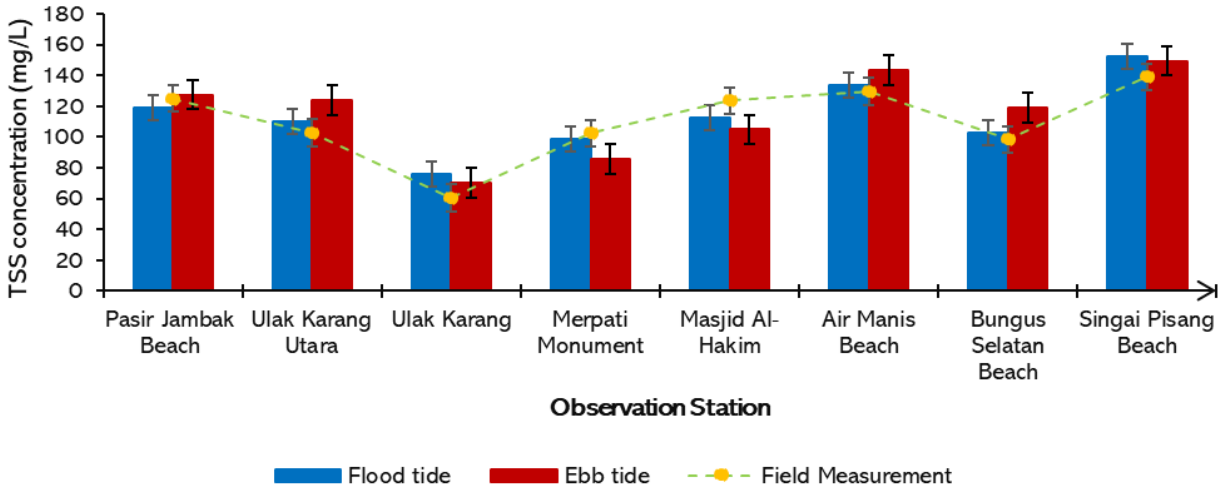


*Source: Analysis, 2022*

**Figure 7.** Estimated TSS concentration during flood and ebb tides validated by the field measurement

The predicted bed level change indicating coastal erosion (sedimentation) (Figure 8) shows that the high value of bed level change is identified in almost all observed subdistricts, with the altered bed level ranging from 0 to -4 m. In contrast, the positive bed level value of 0 – 0.39 m is observed in the southern Koto Tangah, in the middle of Padang Barat, Padang Selatan, and several parts of Bungus Teluk Kabung Subdistrict (Figure 8). This state is consistent with the spatial analysis results (Figures 4 and 5), where coastal instability on Padang Coastline occurs.

The changes in bed level reflect the wave-current-induced bed shear stress. Spatially, the level of wave impact depends on the bed elevation (more significant in shallow water) and the existence of coastal protection and vegetation-dissipated wave energy (Burnette & Dally, 2018). The longshore current previously discussed elucidates the high erosion in several vital areas, proven by the high value of bed-level. Integrating bed level changes, estimated sediment transport, and TSS profiles could be a basis for examining the variability in erosion parameters caused by the changes in bed sediment properties (Bayhaqi et al., 2022).

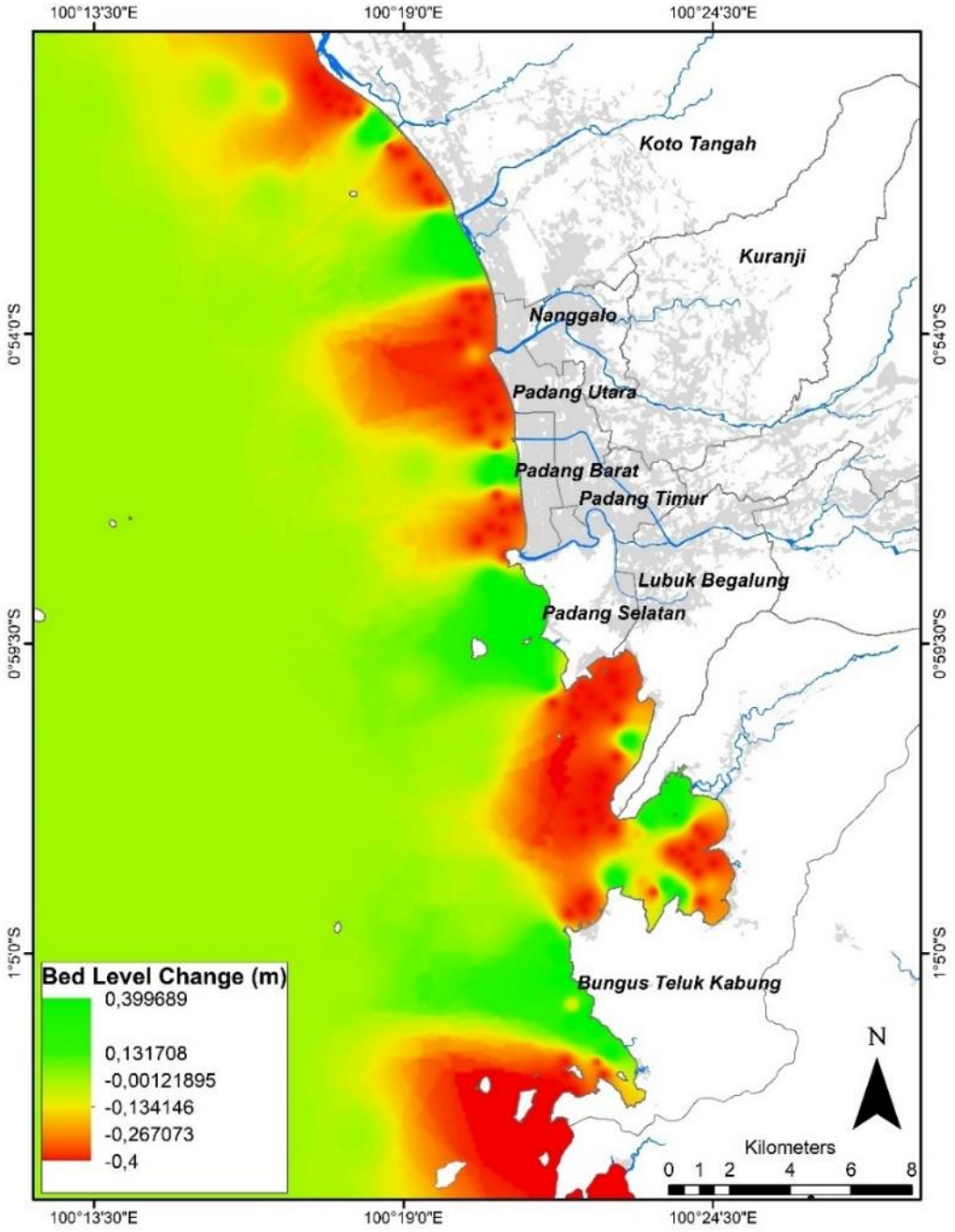


**Figure 8**. Estimated Bed Level Change Indicating Coastal Erosion and Sedimentation in the Padang Coastal Area

Because of the limited oceanographic data collected in this study, we only validate the simulation result using satellite and forecasted tidal data with less than 10% of RMSE (Root Mean Square Error). However, we could compare the TSS modeling result with the filed data collection in 2019 with an adequately close concentration between flood and ebb tides. Long-term field measurement of oceanographical data could enhance the quality of simulation results.

## 4. Conclusion

Padang City's coastline has been experiencing overwhelming coastal erosion with a coastal retreat of about two m/year. The very low to moderate vulnerability is predominant in the northern coastline of Padang City due to the presence of coastal structures. In contrast, high and very high vulnerability is observed on the southern coast. The robust hydrodynamic profiles during September-March allow the higher transport mechanism near the beach. Even though coastal urban development and artificial coastal protection could reduce the impact of hazards and disasters, it does not effectively trap the sediment to stabilize the eroded coastline, thereby inducing erosion in the other areas. The robust hydrodynamic features derived from the Indian Ocean erode the unprotected areas on the southern coast, proven by relatively high sediment transport and turbulence.

It is recommended to reconsider and study the site's oceanographical conditions before constructing a coastal building and developing the coastal area. Even though urban development offers benefits in terms of protection (from hazards and disasters) and tourism, based on this study, it influences the deformation of longshore current pattern-induced sediment transport, thereby inducing coastal instability and erosion. Other nature-friendly solutions, such as a non-woven geotextile, hybrid engineering, and mangrove cultivation, could be a better option to protect the coastal area.

This study only considers 14 parameters to be assessed using a Smartline-associated CVI technique whereby other factors may have a significant influence on determining the coastal vulnerability. Therefore, we recommend evaluating other physical parameters for further studies to get a better depiction of coastal vulnerability. On the other hand, long-term field measurement of tides, currents, and waves is required to understand the study area's real-time oceanographical variability and validate any modeling approaches employed in the future.

## 5. Acknowledgments

We would like to thank Research Institute for Coastal Resources and Vulnerability (RICRV) for the research funding in 2019 in Padang Coastline City with grant number: 032.12.05.2428.003.001.053B and the head of RICRV, Nia Naelul Hasanah Ridwan. Gratitude is also given to local governments (DKP dan Balibangda) of West Sumatra Province for assistance during the field survey and those who have contributed to this work.

## 6. References

Abuodha, P. A. O., & Woodroffe, C. D. (2010). Assessing vulnerability to sea-level rise using a coastal sensitivity index: A case study from southeast Australia. *Journal of Coastal Conservation*, *14*(3), 189–205. [Crossref]

Anwar, H. Z. (2011). Early Warning Function and community Readiness in Reducing the Risk of Tsunami Disaster in Indoensia: Case Study in Padang City. *Jurnal RISET Geologi Dan Pertambangan*, *21*(1). [Crossref]

Bayhaqi, A., Wisha, U. J., & Iswari, M. Y. (2022). The Evidence of Coastline Changes in Banten Bay, Indonesi. *Trends in Sciences*, *19*(4).[Crossref]

Burnette, C., & Dally, W. R. (2018). The Longshore Transport Enigma and Analysis of a 10-Year Record of Wind-Driven Nearshore Currents. *Journal of Coastal Research*, *341*, 26–41. [Crossref]

Dada, O. A., Agbaje, A. O., Adesina, R. B., & Asiwaju-Bello, Y. A. (2019). Effect of coastal land use change on coastline dynamics along the Nigerian Transgressive Mahin mud coast. *Ocean and Coastal Management*, *168*. [Crossref]

Fajri, F., & Tanjung, A. (2012). Abrasion Study Padang Beach, Padang City, West Sumatera Province. *Jurnal Perikanan Dan Kelautan*, *17*(2), 36–42. [Crossref]

Fajrin, F., Almegi, A., Bakari, A., Ramadhan, R., & Antomi, Y. (2021). Enviromental Monitoring of Land Subsidence in The Coastal Area of Padang City Using Sentinel 1 Sar Dataset. *Sumatra Journal of Disaster, Geography and Geography Education*, *5*(1).[Crossref]

Gemilang, W. A., Wisha, U. J., & Rahmawan, G. A. (2018). Particle Size Characteritics of Riverbed Sediments Transported by Tidal Bore 'BONO' in Kampar Estuary, Riau-Indonesia. *Marine Research in Indonesia*, *43*(1), 25–35. [Crossref]

Gemilang, Wisnu A, Wisha, U. J., & Dhiauddin, R. (2020). Coastal Vulnerability Assesment of Tourism Area And Management Srategy for Susstainable Environmental Resilience : Case of Mandeh Coast , West Sumatera. *Majalah Ilmiah Globe*, *22*(1), 1–12.

Gemilang, Wisnu Arya, Husrin, S., Wisha, U. J., & Kusumah, G. (2017). Coastal Vulnerability Due to Landslide Disaster in Bungus, West Sumatera and its surrounding Using Storie Method. *Jurnal Geosaintek*, *3*(1), 37–44. [Crossref]

Gündogan, R., Özyurt, H., & Akay, A. . E. (2011). The effects of land use on properties of soils developed over ophiolites in Turkey. *International Journal of Forest, Soil and Erosion*, *1*(1), 36–42.

Hakam, A., Junaidi, Adji, B. M., & Hape, S. R. (2019). West Sumatra Coastline change due to abrasion protection structures: Padang beach. *International Journal of GEOMATE*, *16*(57). [Crossref]

Haryani, A. I., & Syah, N. (2018). Coastal Abrasion and Accretion Studies of West Sumatera Province in Period 2003-2016. *Journal of Environmental Science and Engineering A*, *7*(7), 1. [Crossref]

Himmelstoss, E. A., Henderson, R. E., Kratzmann, M. G., & Farris, A. S. (2018). Digital Shoreline Analysis System ( DSAS ) Version 5.0 User Guide. In *Open-File Report 2018-1179*.

Jadidi, A., Mostafavi, M. A., Bédard, Y., Long, B., & Grenier, E. (2013). Using geospatial business intelligence paradigm to design a multidimensional conceptual model for efficient coastal erosion risk assessment. *Journal of Coastal Conservation*, *17*(3), 527–543. [Crossref]

Khan, S., Vincent, H., & Wilson, B. (2021). The late Holocene Erin deflected and asymmetric wave-dominated delta – Puerto Grande Bay, Trinidad. *Marine Geology*, *439*. [Crossref]

Koropitan, A. F., Barus, T. A., & Cordova, M. R. (2021). Coastal Water Properties And Hydrodynamic Processes In The Malacca Strait: Case Study Northeastern Coast Of Sumatra, Indonesia. *Journal of Ecological Engineering*, *22*(11), 16–29. [Crossref]

Latief, H. (2012, September). Tsunami Risk Study in the West Sumatera Provinve and Its Mitigation Efforts. *Proceedings PIT HAGI 2012*.

Lins-de-Barros, F. M., & Muehe, D. (2013). The smartline approach to coastal vulnerability and social risk assessment applied to a segment of the east coast of Rio de Janeiro State, Brazil. *Journal of Coastal Conservation*, *17*(2), 211–223. [Crossref]

Mandal, S., Sil, S., Gangopadhyay, A., Jena, B. K., & Venkatesan, R. (2020). On the nature of tidal asymmetry in the Gulf of Khambhat, Arabian Sea using HF radar surface currents. *Estuarine, Coastal and Shelf Science*, *232*. [Crossref]

Nurdjaman, S., & Putra, P., A. (2017). Numerical Simulation of Bed Level Changes Around Structure Due to Waves and Current. *Journal of Civil Engineering*, *24*(3), 199–208. [Crossref]

Oktiari, D., & Manurung, S. (2010). Model Geospasial Potensi Kerentanan Tsunami Kota Padang. *Jurnal Meteorologi Dan Geofisika*, *11*(2), 140–146. [Crossref]

Pascolo, S., Petti, M., & Bosa, S. (2018). On the wave bottom shear stress in shallow depths: The role ofwave period and bed roughness. *Water (Switzerland)*, *10*(10). [Crossref]

Putri, Y. P., Barlian, E., Dewata, I., & Al, T. T. (2018). Policy Instruction of Flood disaster Mitigation in Kuranji Watershed, Padang City. *Majalah Ilmiah Globe*, *20*(2), 87–98. [Crossref]

Ramdhan, M. (2021). Coastal Vulnerability Impacts and Adaptations in Padang City, West Sumatera Province. *Indonesian Journal of Earth Sciences*, *1*(1), 1–9.[Crossref]

Rizal, A. M., & Ningsih, N. S. (2020). Ocean wave energy potential along the west coast of the Sumatra island, Indonesia. *Journal of Ocean Engineering and Marine Energy*, *6*(2), 137–154. [Crossref]

Roy, S., Mahapatra, M., & Chakraborty, A. (2018). Shoreline change detection along the coast of Odisha, India using digital shoreline analysis system. *Spatial Information Research*, *26*(5), 563–571. [Crossref]

Sharples, C., Mount, R., Pedersen, T., Lacey, M., Newton, J., Jaskierniak, D., & Wallace, L. (2009). *The Australian coastal smartline geomorphic and stability map version 1: project report*.

Tanto, T. Al, Putra, A., & Yulianda, F. (2017). Ecotourism feasibility in Pasumpahan Island, Padang City. *Majalah Ilmiah Globe*, *19*(2), 135–146. [Crossref]

Thom, B. G., Eliot, I., Eliot, M., Harvey, N., Rissik, D., Sharples, C., Short, A. D., & Woodro, C. D. (2018). National sediment compartment framework for Australian coastal management. *Ocean and Coastal Management*, *154*(January), 103–120. [Crossref]

Tohari, A., Sugianti, K., & Soebowo, E. (2011). Liquefaction Potential at Padang City: A Comparison of Predicted and Observed Liquefactions During the 2009 Padang Earthquake. *Jurnal RISET Geologi Dan Pertambangan*, *21*(1), 1–7. [Crossref]

Triatmodjo, B. (2012). *Perencanaan Bangunan Pantai* (2nd ed.). Beta Offset Yogyakarta.

Wardani, A., Besperi, besperi, & Gunawan, G. (2019). Modeling Coastaline Changes Using Genesis in the Coastal Area of Padang City. *Seminar Nasional Inovasi, Teknologi Dan Aplikasi (SeNITia) 2019*, 138–143.

Wentworth, C. K. (1922). A scale of grade and class terms for clastic sediments. *Journal of Geology*, *30*(5), 377–392.

Wisha, U. J., Dhiauddin, R., Rahmawan, G. A., & Wijaya, Y. J. (2021). Preliminary identification of causes to local coral bleaching event in manjuto beach, pesisir selatan regency, west sumatra: A hydro-oceano-graphic perspective. *Jurnal Ilmiah Perikanan Dan Kelautan*, *13*(2), 156–170. [Crossref]

Wisha, U. J., Tanto, T. A., Pranowo, W. S., & Husrin, S. (2018). Current movement in Benoa Bay water, Bali, Indonesia: Pattern of tidal current changes simulated for the condition before, during, and after reclamation. *Regional Studies in Marine Science*, *18*, 177–187. [Crossref]

Wisha, U. J., Wijaya, Y. J., & Hisaki, Y. (2022a). Real-Time Properties of Hydraulic Jump off a Tidal Bore, Its Generation and Transport Mechanisms: A Case Study of the Kampar River Estuary, Indonesia. *Water (Switzerland)*, *14*(16), 2651. [Crossref]

Wisha, U. J., Wijaya, Y. J., & Hisaki, Y. (2022b). Tidal bore generation and transport mechanism in the Rokan River Estuary, Indonesia: Hydro-oceanographic perspectives. *Regional Studies in Marine Science*, *52*. [Crossref]

Yuhendra, R., Suriani, R., Umar, Z., & Anggraini, L. (2019, November). Coastal Abrasion in Air Manis Beach, Padang City, the Cause and Control Efforts. *Pertemuan Ilmiah Tahunan 36 Himpunan Ahli Teknik Hidraulik Indonesia*.

Zhu, Q., van Prooijen, B. C., Wang, Z. B., & Yang, S. L. (2017). Bed-level changes on intertidal wetland in response to waves and tides: A case study from the Yangtze River Delta. *Marine Geology*, *385*. [Crossref]